Environmental Earth Sciences (2022) 81:213
https://doi.org/10.1007/s12665-022-10341-9

ORIGINAL ARTICLE

Environmental and health impact of current uranium mining activities in southwestern Sinai, Egypt

Randa S. Ramadan[1] · Yehia H. Dawood[1] · Mohamed M. Yehia[2] · Ahmed Gad[1]

Received: 24 August 2021 / Accepted: 9 March 2022 / Published online: 29 March 2022

Abstract

Stream sediments and groundwater samples were collected from the vicinity of El Allouga uranium mine in southwestern Sinai and analyzed for their radionuclides to explore the geochemical dispersion and environmental impact. The radioactivity measurements were performed using γ-ray spectrometry and UV-photometry. Most stream sediments samples have eU concentrations more than the background level. The significant correlations between eU, clay, and organic matter contents reflect possible adsorption of U to the surface of clay and organic matter. The high radionuclide concentrations in the stream sediment are mainly due to contamination from the mining process, and, in some locations, due to rock outcrops weathering. The measured concentrations of U in groundwater samples exceed the Maximum Contamination Level of groundwater U (30 ppb). The lack of correspondence of U concentrations in the country rocks and associated groundwater indicates the high mobility of U and reflects absence of a simple rock/water equilibration. Water resources in the study area have $^{234}U/^{238}U$ activity ratios with obvious deviations from secular equilibrium. The U isotopic data support that uranium ore body could be locally forming within the rock aquifer at El Allouga area. The calculated external hazard parameter values are higher than the worldwide average in 30% of the studied stream sediment samples; this indicates that people who are exposed to that level of radiation for a lifetime would have an elevated cancer risk. The Annual Effective Dose resulting from U activity concentrations in the studied drinking water is significantly higher than the recommended limit for children and adults. Therefore, the available water resources in the study area are considered unsafe for human consumption.

Keywords Stream sediments · Southwestern Sinai · Radioactivity · Uranium mining · Health hazard

Introduction

To expand the energy resources, Egypt started to renew its ambitious plan to build reactors to generate electricity. Sixty-three years (1956–2019) of intensive uranium exploration and exploitation led to the discovery of a number of radioactive anomalies. Evaluation and mineral processing activities were focused on the black sand deposits of the northern Nile River delta as a non-conventional resource for uranium and thorium, as well as uranium deposits in Sinai and Eastern Desert regions (NEA 2004). Out of several uranium-bearing mineralized zones, two uranium deposits have been mined: Gabal Gattar postorogenic granites in the Eastern Desert and the Paleozoic sedimentary rocks at Gabal Allouga in southwestern Sinai. Most uranium occurrences in Egypt have low-grade uranium ores which can be separated by leaching techniques (Abdel-Monem et al. 1996; NEA 2014).

Uranium mining and milling (UMM) release considerable amounts of natural radionuclides and toxic metals, originally detained in the unexploited uranium deposits. Groundwater, soil, stream sediments, and the atmosphere generally receive contaminations from these harmful substances (Benes 1999; Hanfi 2019; Blake et al. 2020; Borges et al. 2021). In addition to radiotoxicity, uranium, as a heavy metal has a

✉ Ahmed Gad
A.gad@sci.asu.edu.eg; gadahmed67@yahoo.com

Randa S. Ramadan
randaramadan@sci.asu.edu.eg

Yehia H. Dawood
yhdawood@sci.asu.edu.eg; yhdawood@yahoo.com

Mohamed M. Yehia
drmohamedmokhtar160@gmail.com

[1] Geology Department, Faculty of Science, Ain Shams University, Cairo 11566, Egypt

[2] Central Laboratory for Environmental Quality Monitoring, National Water Research Center, El Qanater, Egypt

fatal chemotoxicity. Humans' exposure to uranium mainly occurs via water drinking, food ingestion and inhalation (Ma et al. 2020). The main chemical effect associated with exposure to uranium and its compounds is kidney toxicity (Craft et al. 2004). Nevertheless, a considerable amount of uranium that enters the body gets distributed to different organs where it can have long-term effects.

Uranium ore exploration and mining activities at El Allouga area started in 1957. Currently, mining process comprises both open-pit and underground operations, with mineral processing carried out on the site. The ore is processed by crushing, grinding, and leaching with sulphuric acid, followed by ion-exchange process and then precipitation of uranium using sodium hydroxide. A large quantity of mine tailings in the form of slurry waste are placed in small piles adjacent to the mine without engineered barriers. The waste is represented mainly by fine-grained tailings left on site (Harpy et al. 2019). Most of this waste and residues were disposed in the near-surface impoundments in the surrounding area of the mines. During the processing, no safety measures were taken to assure the isolation of the tailings from the environment. The major threat of these tailings is the leaching of contaminants (e.g., radionuclides and heavy metals) into groundwater which is considered the main source of drinking water in the area. Due to the mountainous topography with steep slopes, the incidence of seasonal floods and rainy episodes are common. These episodes largely affect or even destroy some of the tailing's piles. The inappropriate management of the mining process in El Allouga have caused a deleterious impact on the environment in the southeastern Sinai region, especially on the quality of the drinking water and stream sediments (Aboelkhair and Rabei 2012; Korany et al. 2013; El-Aassy et al. 2015).

Southeastern Sinai wadis are inhabited with indigenous community who are principally affected by the mining operation. Uranium mining areas around the world also affected indigenous people, including the tribal groups in Africa such as Imouraren uranium mine in Niger, native Americans in North America such as Ross-Adams mine in Alaska and aborigines in Australia such as Ranger mine in the northern territory and Olympic Dam mine in the south (Downing et al. 2002; Blake et al. 2015; Hund et al. 2015; Lewis et al. 2017; Winde et al. 2017; Schultz 2021). Over the past few years, several studies have been carried out in southwestern Sinai to investigate the environmental impact of uranium mineralization in the exposed rocks (El Galy et al. 2008; El Aassy et al. 2011; Abd El-Halim et al. 2017; Khattab et al. 2017), surface deposits (Aboelkhair and Rabei 2012; Korany et al. 2013), groundwater (El Aassy et al. 2015) and to enforce a proper dose limitation system for workers (Abdel-Monem et al. 1996). These studies provided valuable data about the environmental radioactivity situation in southwestern Sinai. The shortcoming of these studies is that most of them were conducted dealing with small scale (single wadi). The age-dependent dose assessment due to ingestion of uranium from the consumption of drinking water was nonetheless not considered in any of the previous studies.

The present study aimed to investigate the ^{238}U, ^{234}U, ^{232}Th, and ^{40}K isotopic composition of stream sediments and groundwater located nearby El Allouga mining area and to identify the factors influencing the distribution of these radionuclides, moreover, to quantify the long-term effects of the current uranium mining activities in the area and assess the potential external radiation exposure of humans and internal dose assessment from the consumption of drinking water.

Materials and methods

Study area

The study area is located in southwestern Sinai about 40 km east of Abu Zeneima town between longitude 33° 18′–33° 26′ E and latitude 28° 57′ 30″–29° 5′ N. This area is characterized by the presence of many economic ore deposits especially cupper, manganese and uranium ores (Hussein et al. 1992). This study includes four main wadis (Wadi Nasieb, Wadi El Seih, Wadi Baba, and Wadi El Sahu) (Fig. 1). These wadis are inhabited by Bedouin communities that used natural materials and available resources in their living system.

Geology and mineralization

The area under consideration is covered by Precambrian crystalline basement rocks which are non-conformably overlain by Paleozoic sedimentary rocks (Fig. 2) ranging in age from Cambro-Ordovician to Carboniferous and achieve a thickness ranging from 212 to 375 m (Abdel-Monem et al. 1996). The Precambrian rocks encompass gneisses, schists, diorites, granodiorites, granitic bodies and migmatites. The Paleozoic rocks comprise seven formations starting with the Cambrian rocks Sarabit EI Khadem, Abu Hamata, and Adediya Formations which are unconformably overlain by the Um Bogma Formation (lower Carboniferous). The latter is conformably overlain by El Hashash, Magharet El–Mayah, and Abu-Zarab Formations (Aboelkhair and Rabei 2012).

The Um Bogma Formation is the most significant among the Paleozoic sedimentary rocks in southeastern Sinai since it contains the Fe–Mn, Cu, and U mineralization (Hussein et al. 1992). It is subdivided into three members Ras Samra Member (lower shaly-ore Member), EI-Qor Member (middle marly dolostone–siltstone Member), and Um Shebba Member (upper dolostone Member) (Kora et al. 1994). This formation consists of many sedimentary facies: gibbsite-bearing sediments, claystone, shale, ferruginous siltstone, marl, dolostone, and Mn–Fe ore.

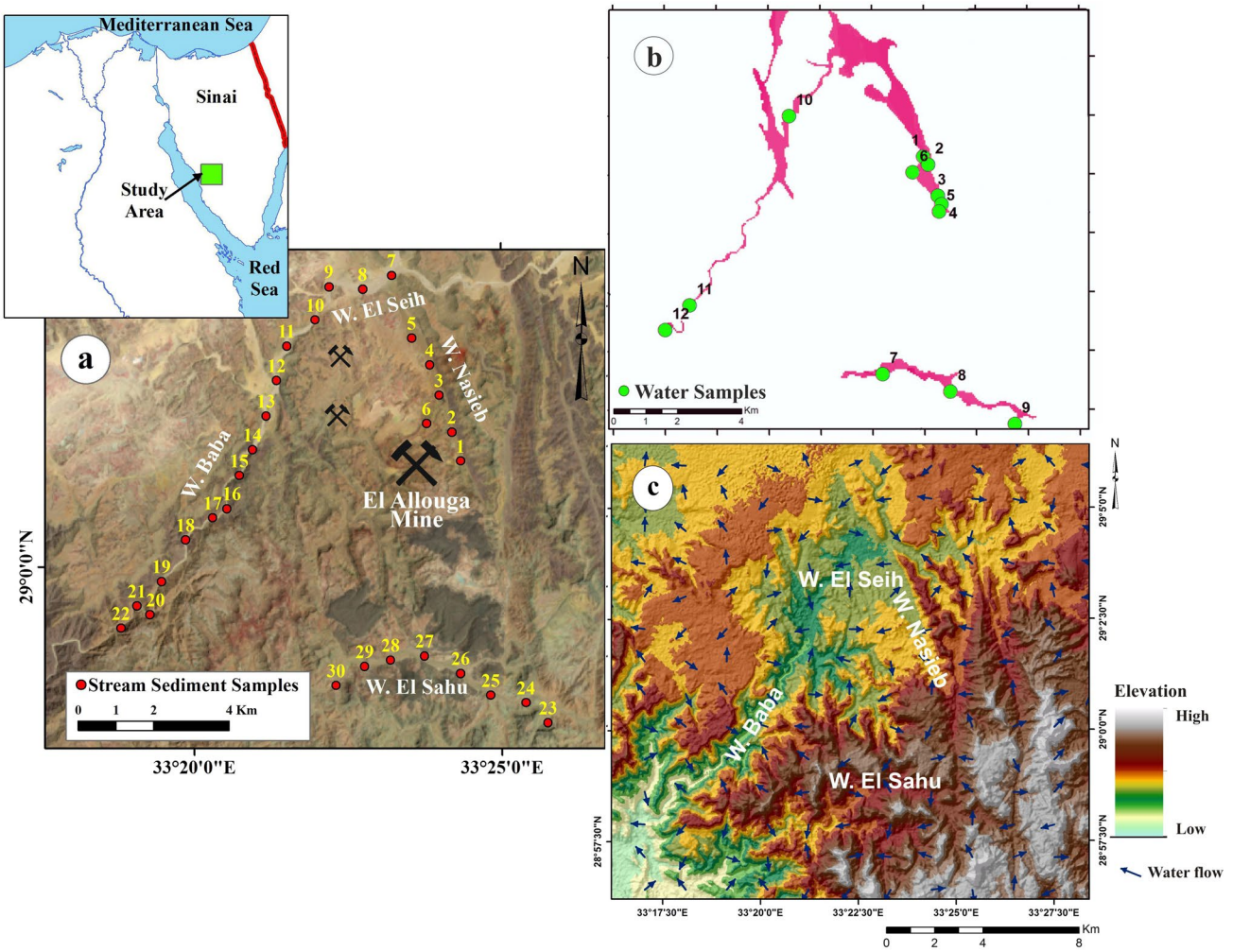

Fig. 1 Map displaying the study area, stream sediments sampling locations (**a**), water sample locations (**b**), and digital elevation model (DEM) of the study area (**c**)

The U-minerals are hosted in the dolostone, siltstone, shale, and claystone especially in Ras Samra Member. These minerals include U-oxides (Uraninite, Coffinite, Brannerite), uranyl-oxyhydroxides (Clarkeite, Metacalciouranoite, Liebigite), uranyl silicates (Uranophane, Beta-Uranophane, Kasolite, Sklowdowskite, Boltwoodite, Soddyite), phosphates (Autunite, Meta-Autunite, Sodium Meta-autunite, Meta-torbernite, Bassetite, phurcalite, Uranphite, Meta-uranocircite, Phosphuranylite, Renardite), arsenates (Meta-zeunerite), vanadates (Carnotite, Rb-Carnotite, Meta-tyuyamunite, Strelkinite), molybdates (Moluranite, Sedovite, Umohoite), and sulfates (Zippeite, K-Zippeite, Zn Zippeite, uranopilite) (Hussein et al. 1992; Alshami 2018). These minerals association indicates formation under oxidizing conditions with pH values range (6–7.5) and a high evaporation rate (Alshami 2018). On the other hand, many detrital and uranium-bearing minerals were identified such as xenotime, monazite, zircon, atacamite, and jarosite (Hussein et al. 1992; Ramadan et al. 2019).

Sampling and preparation

A total of 47 samples were collected from the study area. They represent 30 stream sediments samples that were collected from 4 wadis (Wadi Nasieb, Wadi El Seih, Wadi Baba, and Wadi El Sahu) and 12 water samples from the available water resources (10 groundwater and 2 surface water samples) (Fig. 1). In addition, five samples were collected representing the country rocks of some drilled wells in the study area. The exact locations of the sample sites (Longitudes and Latitudes) were recorded using Geographical Positioning System (GPS). The stream sediment samples were collected by a clean stainless-steel shovel from one joint sampling site of a 5 m^2 square. Samples are composed of subsamples of approximately equal volume, taken at up

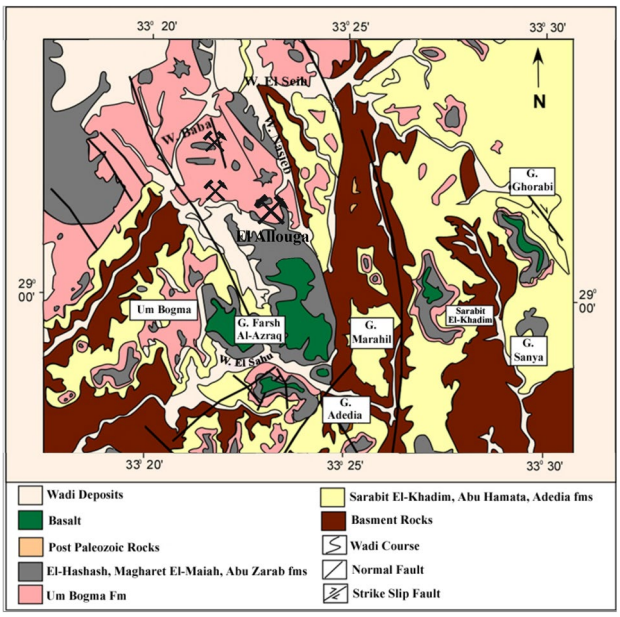

Fig. 2 Geologic map of Abu Zeneima area

to a 50 cm depth from each angle and from the center of this square. They were packed in polyethylene bags, transferred to the laboratory and stored at room temperature. On the other hand, the water samples (2 L) were collected in pre-cleaned polyethylene containers. On-site measurement of pH was carried out at the site of sample collection following the standard protocols and methods adopted by APHA (1995).

After removal of recognizable stones and roots, each sediment sample was dried at room temperature for about 1 week to eliminate moisture. The air-dried soil sample was sieved through a 2 mm sieve before analysis. The samples were split into several parts for different laboratory investigations.

Physico-chemical and mineralogical characteristics

Organic matter contents were measured by loss on ignition following the procedure adopted by Van Reeuwijk (2002). Clay contents were measured and analyzed by the pipette method (Ingram 1971). Heavy fractions were separated from medium, fine, and very fine sand sizes of each sample using the heavy liquid separation technique (Mange and Maurer 1992). Morphological and qualitative chemical composition of selected mineral grains were performed using SEM and EDX techniques available at the Nuclear Materials Authority of Egypt [Model Phillips XL 30].

Chemical analysis

The collected groundwater samples were filtered through 0.45 µm pore-diameter filter paper. The gravimetric method was used to determine TDS (APHA 1995). The concentrations of major ions were determined using Inductively Coupled Plasma-Optical Emission Spectroscopy (ICP-OES) with ultrasonic Nebulizer (USN) (Perkin Elmer Optima 3000, USA) available at the accredited (ISO/IEC 17,025) Central Laboratory for Environmental Quality Monitoring, National Water Research Center.

Radioactivity measurements

The ^{238}U, ^{232}Th, and ^{40} K contents of the stream sediment samples were measured using a Sodium Iodide (NaI) detector. The detector is protected by a copper cylindrical protection (0.6 cm thickness) against induced X-ray and chamber of lead bricks against the environmental radiations and covered by a lead shield (5 cm thickness). Energy calibration of the detector was performed using standard point sources (^{137}Cs and ^{60}Co). Sediment samples were dried, pulverized, homogenized, weighted, and sieved (125 µm mesh size). The meshed samples were transformed into a Marinelli container (100 ml) and sealed for a period of about 4 weeks before analysis. This allows the in-growth of uranium and thorium decay products to prevent the escape of radiogenic gases ^{222}Rn and ^{220}Rn and allowed secular equilibrium between ^{238}U, ^{232}Th, and their daughter products (Hamby and Tynybekov 2000; Gad et al. 2019; Osman et al. 2022). After attainment of secular equilibrium, each sample was counted for 1000 s.

Uranium concentrations in groundwater samples were measured using PC scanning spectrophotometer UV/VIS double beam of the type LABOMED, INC (U.S.A.) available at Nuclear Materials Authority of Egypt. The energy used is from 110 to 220 V and frequency from 50 to 60 Hz. The sample solution (not more than 80 µg of uranium) was placed in a 10 ml volumetric flask, 1.5 ml of arsenazo-III solution was added and mixed well, 0.6 ml of bi-distilled water, and 0.2 ml of NH_4OH solution was added and shaken for 3 min. 4 ml of Urea/HNO_3 solution was then added and the solution was made up to the mark by bi-distilled water. After 5–10 min, the absorbance was measured at λ max 655 nm, using a reagent blank solution as a reference.

To study the uranium series isotopic composition of groundwater, a Hyper-pure Germanium (HPGe) detector EG&G ortec Model GMX60P4 was used with a full width at half maximum (FWHM) of 1.10 keV at the 5.9 keV gamma transition of ^{55}Fe and 2.3 keV at the 1.33 MeV gamma transition of ^{60}Co. The detector has a photo-peak relative efficiency of about 60% of the '3 × 3' NaI (T1) crystal efficiency. The efficiency calibration was performed using (RGU-1, RGTh-1 and RGK-1) reference materials obtained from the International Atomic Energy Agency (IAEA). The detector was shielded to reduce the gamma-ray background by a lead cylinder with a fixed bottom and a movable cover and mounted on a 30-l liquid nitrogen Dewar. The software

program MAESTRO-32 was used to accumulate and analyze the data. 100 ml of each water sample was poured into a Marinelli container and sealed for a period of about 4 weeks. After that, samples were measured for 24 h counting time. The ^{238}U activity concentration was determined indirectly from ^{234}Th and $^{234\,m}$Pa gamma rays at the energy of 63.3 and 1001 keV, respectively. The ^{234}U activity was determined directly from its gamma rays at the energy of 53.2 keV.

Radiation hazard and dose assessment

External radiation hazard

The external radiation hazards susceptibility by wadis inhabitants due to the calculated activity concentrations of A_U, A_{Th}, and A_K in the collected stream sediment samples were assessed by the calculation of the radium equivalent activity (Ra_{eq}), the absorbed dose rate (D), the external annual effective dose (AED_{ex}), and the excess lifetime cancer risk (ELCR).

Dose assessment

To assess the radiological effect of the determined total uranium concentrations in the groundwater samples, the internal annual effective dose (AED_{in}) due to ingestion of U from the consumption of water was calculated for different age groups: infants of 1–3 years, children of 5–18 years and adults above 18 years. The formulae used for calculating the various external and internal parameters are summarized in Table 1.

To specify and outline the research problems, procedures and approach, a conceptual model is constructed as a guide for the main steps in this study (Fig. 3).

Results and discussion

Radionuclides' distribution in the stream sediments

The concentrations of the investigated natural radionuclides and descriptive statistics of the four wadis are reported in Table 2. eU concentrations range from 2 to 9 ppm, 2 to 4 ppm, 1 to 7 ppm, and 2 to 13 ppm, in Wadi Nasieb, Wadi El Seih, Wadi Baba, and Wadi El Sahu, respectively. eTh concentrations in Wadi Nasieb and El Seih are very low. The measured eTh values in the sediments of these two wadis are UDL except sample no. 6 of Wadi Nasieb (3 ppm eTh). In Wadi Baba eTh values range from 1 to 5 ppm, while in Wadi El Sahu range from 10 to 16 ppm. On the other hand, ^{40} K concentration ranges from 0.19 to 0.9%, 0.56 to 1.04%, 0.02 to 0.58%, and 1.38 to 2.87%, in Wadi Nasieb, Wadi El Seih, Wadi Baba, and Wadi El Sahu, respectively.

Normalized to the averages of earth's crust (Taylor 1964), the obtained data revealed that most of the studied sediments have uranium, thorium, and potassium concentrations more than these averages (2, 10, 1.8 ppm, respectively; Taylor 1964) (Figs. 4, 5, 6).

Generally, the impact of mining process is reflected in uranium concentrations of the stream sediments. The results show that the sediments of the closest wadi to the mining area namely, Wadi Nasieb has high contents of uranium. In addition, the samples collected close to the mining area in the different wadis show high uranium contents. For example, sample number 6 in Wadi Nasieb has the highest U content. In addition, sample 10 of Wadi Baba is the closest sample to the mine and show the highest uranium content in this wadi (Fig. 1, Table 2).

Table 1 Summary of the formulae used to calculate the external and internal radiation hazard

S/N	Radiological parameters	Units	Formula
1	Radium equivalent activity (Ra_{eq})	Bq kg^{-1}	$Ra_{eq} = A_U + 1.43A_{Th} + 0.077A_K$[a]
2	Absorbed dose rate (D)	nGy h^{-1}	$D = 0.462A_U + 0.604A_{Th} + 0.0417A_K$[b]
3	External annual effective dose (AED_{ex})	mSv yr^{-1}	$AED_{ex} = D \times T \times DCF \times F_O \times 10^{-6}$[b]
4	Excess lifetime cancer risk (ELCR)	–	$ELCR = AED \times DL \times RF$[c]
5	Internal annual effective dose (AED_{in})	mSv yr^{-1}	$AED_{in} = C_U \times WI \times DCI \times 10^{-6}$[d]

A_U, A_{Th} and A_K are the activity concentrations of uranium, thorium and potassium in the stream sediments (Bq kg^{-1}), respectively. T is time being 8760 h y^{-1}, DCF is external dose conversion factor (0.7 SvG y^{-1}), F_O is outdoor occupancy factors of 0.2 (UNSCEAR 2000). DL is duration of life (70 years) and RF is external risk factor used for public by ICRP (1990) as 0.05 Sv^{-1}. C_U is the activity concentration of uranium in water (Bq l^{-1}), WI is annual intake of drinking water of 150, 350 and 750 L y^{-1} for infants, children and adults, respectively (WHO 2011), DCI is uranium ingestion conversion factor of 1.2×10^{-8}, 6.8×10^{-8} and 4.5×10^{-8} Sv Bq^{-1} for infants, children and adults, respectively (IAEA 1996)

[a]Beretka and Mathew (1985)

[b]UNSCEAR (2000)

[c]Taskin et al. (2009)

[d]ICRP (2012)

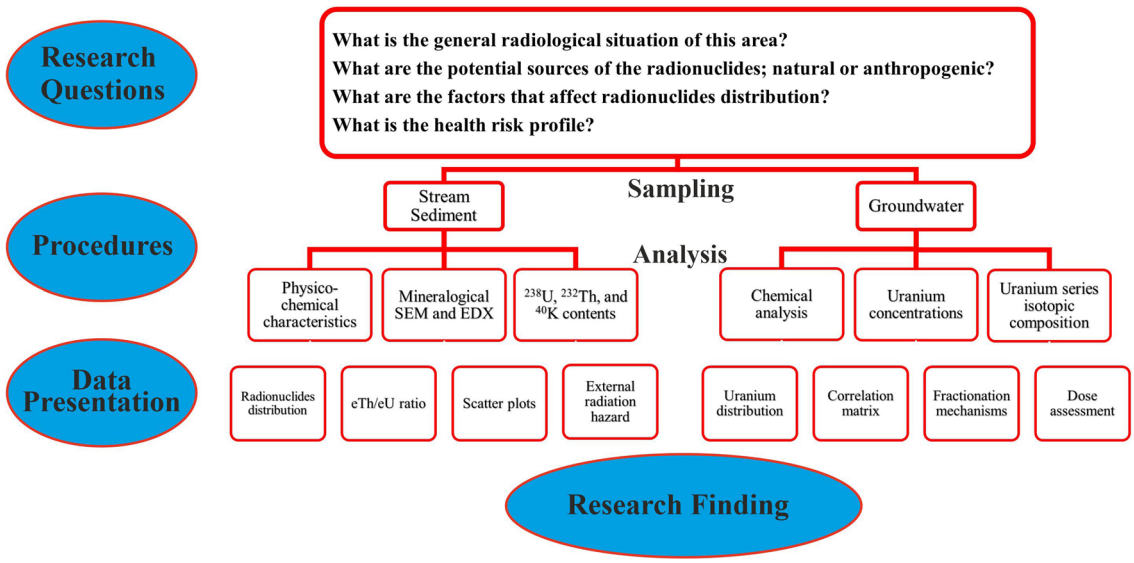

Fig. 3 A conceptual model representing research problems and main steps

Conversely, high concentrations of radionuclides are also reported from the weathering of rock outcrops in Wadi El Sahu. This wadi lies to the south of the mining area but is topographically high and not receiving contamination from the mining area. The elevated concentrations of U, Th, and ^{40}K in the stream sediments of Wadi El Sahu may be attributed to the weathering of the nearby granitic rocks which are considered the main source of radioactivity in the study area. Such trends of these high radioactive concentrations were also reported inextricably associated with granitic exposures in Gabal El Seila area (Abdel-Razek et al. 2016), Abu-Rusheid, Nugrus area, (El-kameesy et al. 2015), Gabal Rei El-Garrah area, Eastern Desert (El Mezayen et al. 2017), and in stream sediments around Sharm El-Sheikh, South Sinai (Heikal et al. 2013; Al-Sharkawy et al. 2012).

In addition to the radionuclides contamination in the studied stream sediments, heavy metals contamination was also reported by Refaei et al. (2019). They reported high concentrations of Cd, Co, Cu, Mn, Ni, Pb, V, and Zn in Wadi Nasieb stream sediments. According to the same authors, the concentrations of Cd, Cu, Mn, Ni, Pb, and Zn are above phytotoxic limits in the sediments of Wadi Nasieb and its surroundings.

eTh/eU ratio

eTh/eU ratio is indicative for the relative depletion or enrichment of radionuclide (Orgün et al. 2007). Uranium enrichment can be indicated by the ratio decrease lower than 3, while uranium leaching out can be indicated by its increase above 3. In the study area, the average of eTh/eU ratio of all wadis is less than Clark's value of 3.5 which indicate enrichment of uranium in the sediments of the studied wadis. In addition, the presence of some uranium and thorium minerals and/or U–Th-bearing minerals in the study area (autunite, uranophane, beta-uranophane, uranium oxide, thorite, thorianite, zircon, monazite, allanite, xenotime, and fergusonite) contribute to the radioactivity of the stream sediments (Guagliardi et al. 2013; Abu-zeid et al. 2017; Ramadan et al. 2019). The bivariant plot (Fig. 7) between eU and eTh of the stream sediments of Wadi El Sahu and Wadi Baba showed a clear gap in eTh contents. The higher eTh contents in Wadi El Sahu reflect additional contribution from Th-bearing minerals from the nearby granitic exposures (Fig. 8).

Factors influencing radionuclides' distribution in the stream sediments

The distribution of radionuclides (U, Th, and ^{40}K) depends mainly on the mechanical and chemical weathering. Mechanical weathering plays an important role in the distribution of Th and ^{40}K, while U is strongly released during intensive chemical weathering under humid climate (Abu-zeid et al. 2017). Throughout the chemical weathering processes, the amounts of thorium and potassium released are fairly small whereas, the leaching of uranium being the dominant feature (Ion 2017). This is achieved in Wadi El Sahu where the effect of mechanical weathering overcomes the geochemical decomposition on the distribution of these elements (Figs. 4, 5, 6).

Statistically, bivariate X–Y scatter plots were constructed between different variables including eU, eTh, ^{40}K, clay %, and organic matter contents (OM %) to investigate the possible sources of radionuclides in the studied sediments

Table 2 Concentrations of radioelements in the studied stream sediments and the calculated values of the external radiological hazard parameters

S. N.	Clay %	OM %	eU		eTh		40K		eTh/eU	Ra_{eq}	D_{ex}	AED_{ex}	ELCR × 10–3
			ppm	Bq kg−1	ppm	Bq kg−1	%	Bq kg−1					
Wadi Nasieb													
1	0.50	2.20	UDL	UDL	UDL	UDL	UDL	UDL	–	0.00	0.00	0.000	0.000
2	0.00	2.80	2.00	24.80	UDL	UDL	UDL	UDL	–	24.80	11.46	0.014	0.098
3	0.00	3.50	5.00	62.00	UDL	UDL	UDL	UDL	–	62.00	28.64	0.035	0.246
4	3.45	1.70	4.00	49.60	UDL	UDL	UDL	UDL	–	49.60	22.92	0.028	0.197
5	0.00	3.00	2.00	24.80	UDL	UDL	0.60	187.80	–	39.26	19.29	0.024	0.166
6	3.43	4.11	9.00	111.60	3.00	12.18	0.19	59.47	0.33	133.60	61.40	0.075	0.527
Wadi El Seih													
7	3.00	3.20	UDL	UDL	UDL	UDL	0.87	272.31	–	20.97	11.36	0.014	0.097
8	2.30	1.90	4.00	49.60	UDL	UDL	0.56	175.28	–	63.10	30.22	0.037	0.259
9	0.70	3.50	2.00	24.80	UDL	UDL	1.04	325.52	–	49.87	25.03	0.031	0.215
Wadi Baba													
10	2.73	2.50	7.00	86.80	UDL	UDL	UDL	UDL	–	86.80	40.10	0.049	0.344
11	4.50	4.80	2.00	24.80	2.00	8.12	0.32	100.16	1.00	44.12	20.54	0.025	0.176
12	0.81	2.70	3.00	37.20	2.00	8.12	UDL	UDL	0.67	48.81	22.09	0.027	0.190
13	0.00	2.70	3.00	37.20	2.00	8.12	0.02	6.26	0.67	49.29	22.35	0.027	0.192
14	2.30	1.00	4.00	49.60	3.00	12.18	UDL	UDL	0.75	67.02	30.27	0.037	0.260
15	2.50	2.60	3.00	37.20	4.00	16.24	0.25	78.25	1.33	66.45	30.26	0.037	0.260
16	2.32	1.70	3.00	37.20	4.00	16.24	0.32	100.16	1.33	68.14	31.17	0.038	0.268
17	3.40	4.20	3.00	37.20	4.00	16.24	0.26	81.38	1.33	66.69	30.39	0.037	0.261
18	0.00	2.90	5.00	62.00	4.00	16.24	0.17	53.21	0.80	89.32	40.67	0.050	0.349
19	3.63	2.70	3.00	37.20	4.00	16.24	0.04	12.52	1.33	61.39	27.52	0.034	0.236
20	2.50	0.70	2.00	24.80	1.00	4.06	UDL	UDL	0.50	30.61	13.91	0.017	0.119
21	3.00	2.20	1.00	12.40	2.00	8.12	0.58	181.54	2.00	37.99	18.20	0.022	0.156
22	0.84	0.02	3.00	37.20	5.00	20.30	0.18	56.34	1.67	70.57	31.80	0.039	0.273
Wadi El Sahu													
23	1.85	0.02	4.00	49.60	16.00	64.96	1.81	566.53	4.00	186.12	85.78	0.105	0.736
24	1.64	2.10	4.00	49.60	13.00	52.78	2.87	898.31	3.25	194.25	92.25	0.113	0.792
25	3.76	2.60	4.00	49.60	14.00	56.84	2.84	888.92	3.50	199.33	94.31	0.116	0.810
26	1.60	1.90	5.00	62.00	13.00	52.78	2.39	748.07	2.60	195.08	91.72	0.112	0.787
27	1.07	0.70	2.00	24.80	12.00	48.72	1.38	431.94	6.00	127.73	58.90	0.072	0.506
28	2.00	2.10	2.00	24.80	15.00	60.90	1.94	607.22	7.50	158.64	73.56	0.090	0.632
29	5.35	9.70	13.00	161.20	10.00	40.60	1.62	507.06	0.77	258.30	120.14	0.147	1.031
30	3.80	4.20	4.85	60.14	15.66	63.58	2.76	863.88	3.23	217.58	102.21	0.125	0.877
Min	0.00	0.02	1.00	12.40	1.00	4.06	0.02	6.26	0.33	0.00	0.00	0.000	0.000
Median	2.30	2.60	3.00	37.20	4.00	16.24	0.59	184.67	1.33	66.57	30.27	0.037	0.260
Max	5.35	9.70	13.00	161.20	16.00	64.96	2.87	898.31	7.50	258.30	120.14	0.147	1.031
Mean	2.10	2.67	3.89	48.21	7.08	28.74	1.05	327.37	2.12	92.25	42.95	0.053	0.369
Std. deviation	1.48	1.77	2.45	30.41	5.44	22.09	0.99	308.63	1.89	68.24	31.94	0.039	0.274

UDL under detection limit

(Fig. 9). These plots have decisively showed that eU is positively correlated with clay % ($R = 0.493$) and OM % ($R = 0.678$) reflecting adsorption of uranium to the surface of clay minerals and organic matter. On the other hand, the corresponding correlations with eTh and ^{40}K are insignificant indicating a minor role of clay and OM % in the distribution of these two radionuclides.

Uranium also precipitated as uranyl minerals on the surface of iron oxides. The U–FeO association is observed in the source rocks of Um Bogma Formation at Um Hamd

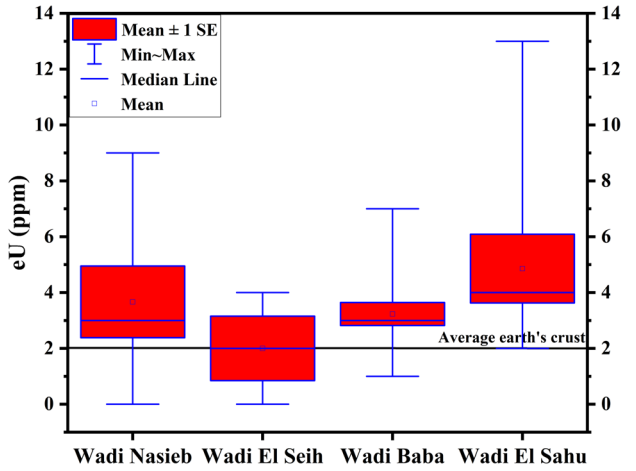

Fig. 4 Boxplot of the eU concentrations in the studied stream sediments

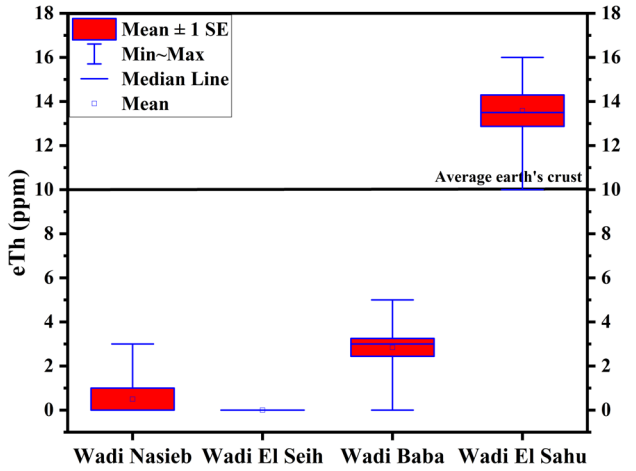

Fig. 5 Boxplot of the eTh concentrations in the studied stream sediments

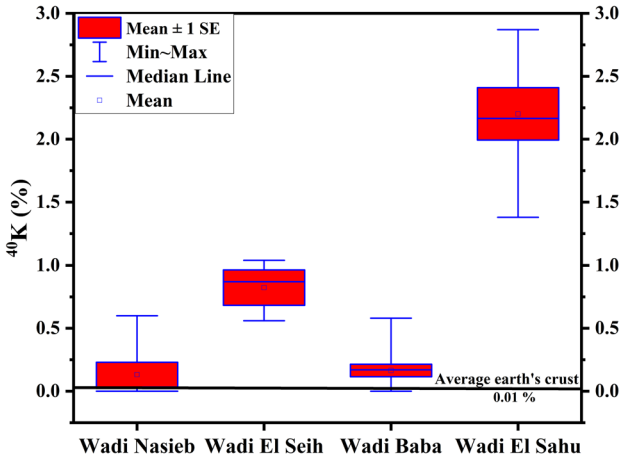

Fig. 6 Boxplot of the ^{40}K concentrations in the studied stream sediments

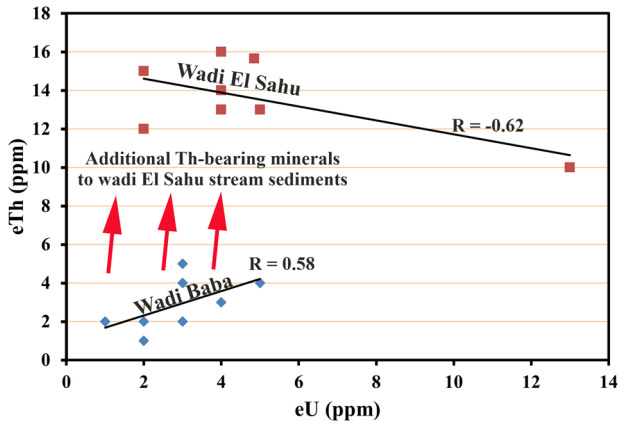

Fig. 7 eTh enrichment in Wadi El Sahu stream sediments. A probable indication for additional Th-bearing minerals in Wadi El Sahu stream sediments from the nearby granitic exposures

locality (Fig. 10). BSE image and EDX pattern (Fig. 8a) show autunite precipitation on colloidal iron oxides.

Distribution of uranium in groundwater

Uranium concentrations, pH, TDS, major ion concentrations and $^{234}U/^{238}U$ activity ratios in the studied water samples are shown in Table 3. The concentrations of uranium in the water samples range from 90 to 1130 ppb with an average value of 517.5 ppb. Spatial distribution map of U concentration (Fig. 11) revealed that the highest U concentration is found at Wadi Baba in the surface water samples 11 and 12 (600, 1130 ppb, respectively). These high concentrations are most probably due to the evaporation effect. The obtained data revealed that all samples are found to exceed the Maximum Contamination Level (MCL) of groundwater uranium (30 ppb) according to (WHO 2011) (Fig. 12). Not only groundwater uranium from the study area is of high concentration, but heavy metals such as Cd and Pb concentrations were reported to be higher than the permissible limit in the water wells from Wadi El Sahu (Hassan et al. 2015). As a consequence, and from the environmental point of view, the available water resources in the study area are considered unsafe for human consumption and irrigation.

Factors influencing uranium distribution in groundwater

Eh and pH are two main factors affect the type of uranium complexes in groundwater (Langmuir 1978). U in the weathering profile is much more soluble and mobile in oxic natural waters. The groundwater from the study area is oxygenated

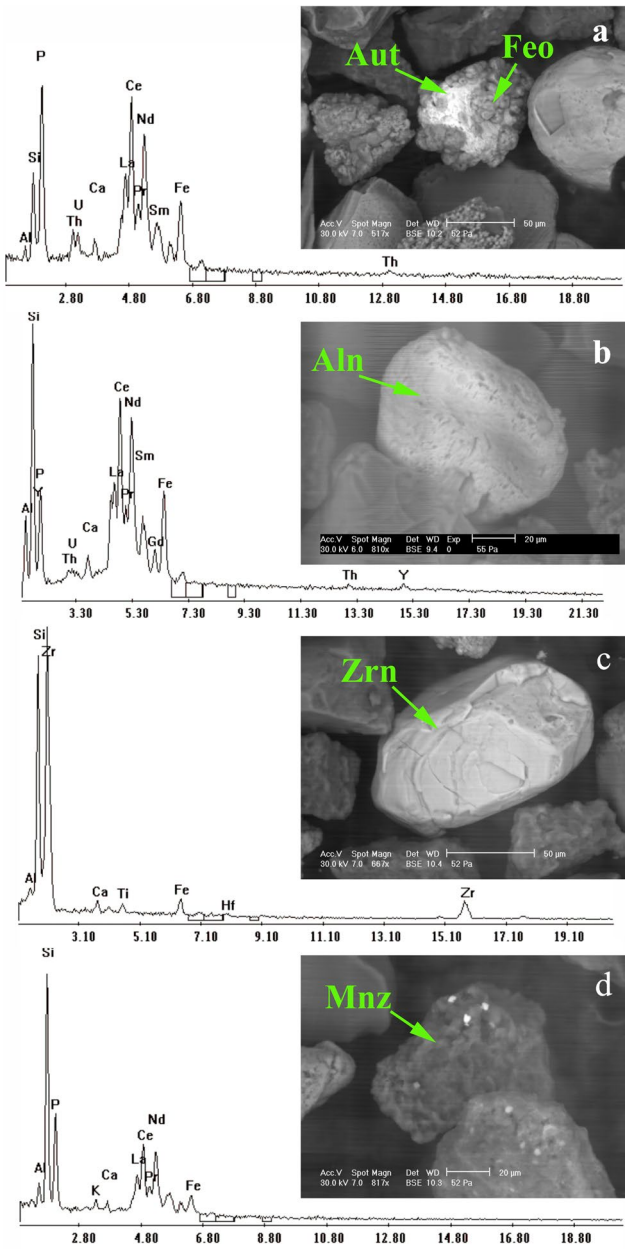

Fig. 8 BSE images and EDX patterns of: **a** encrustation of autunite on colloidal iron oxide mineral grain, **b** allanite grain with surface roughness due to weathering, **c** prismatic zircon grain, **d** minute inclusions of monazite in unidentified silicate mineral

and has pH ranges from 7.9 to 8.2. Therefore, U probably exists in the form of soluble uranyl hydroxides or uranyl bicarbonate complexes (Suzuki and Banfield 1999; Lima et al. 2005).

The correlation matrix between uranium and major ions of the studied groundwater is shown in Table 4. Strong positive correlations are observed between uranium and all major ions. This indicates that the uranium concentration in groundwater increases with increasing its salinity and TDS contents (Fig. 13). Such trend of uranium may be attributed to uranium speciation and adsorption/desorption reactions. Adsorption of uranium can be decreased by coexisting cations due to competition for adsorption sites of the grain surface of minerals (Sturchio et al. 2001). Consequently, the distribution of uranium in the studied groundwater is largely dependent on the high solubility and mobility of this element and on the salinity of the groundwater.

The general lack of correspondence of uranium concentrations in the groundwater and country rocks (Fig. 14) indicates that the high concentrations of uranium in the groundwater are not mainly due to leaching from the nearby country rocks and suggests that the distribution of uranium in these aquifers has multi-sources due to the high mobility of this element.

Fractionation mechanisms in the $^{234}U/^{238}U$ system

The uranium activity ratio ($^{234}U/^{238}U$) has proven to be an influential means in the interpretation of groundwater flow and aquifer interactions (Osmond and Cowart 1992). The activity ratios of uranium isotopes remain constant unless there is a fractionation of isotopes due to natural or anthropogenic activities and this disequilibrium of the $^{234}U/^{238}U$ isotopic ratio in natural waters has been used as a natural tracer tool to identify the uranium source and explore uranium ore deposits (Karpas et al. 2005; El Aassy et al. 2015). In the study area, both surface and subsurface waters have $^{234}U/^{238}U$ activity ratios with obvious deviations from secular equilibrium. The activity ratio ranges from 3.34 to 14 with an average of 5.62, but the average value is biased by the very high activity ratio of sample number 5 from El Allouga drilled well. The majority of the $^{234}U/^{238}U$ activity ratios lie between 3.34 and 5.91 (Table 3; Fig. 15).

The resulting combination of uranium concentration and activity is often a stable fingerprint of water masses and can be used to recognize mixing groundwater sources. If the activity ratio of the dissolved U of a suite of samples in many aquifers is plotted against the reciprocal of U concentration, mixing relations plot as straight lines. The plot of activity ratios vs. reciprocal of U concentration of the studied groundwater (Osmond and Cowart 1992) shows a considerable spread of data and reflects no mixing relations (Fig. 16).

The very high $^{234}U/^{238}U$ activity ratio = 14 (Table 3) in the studied groundwater is observed at El Allouga drilled well (sample 5, located at the uranium mining area). This

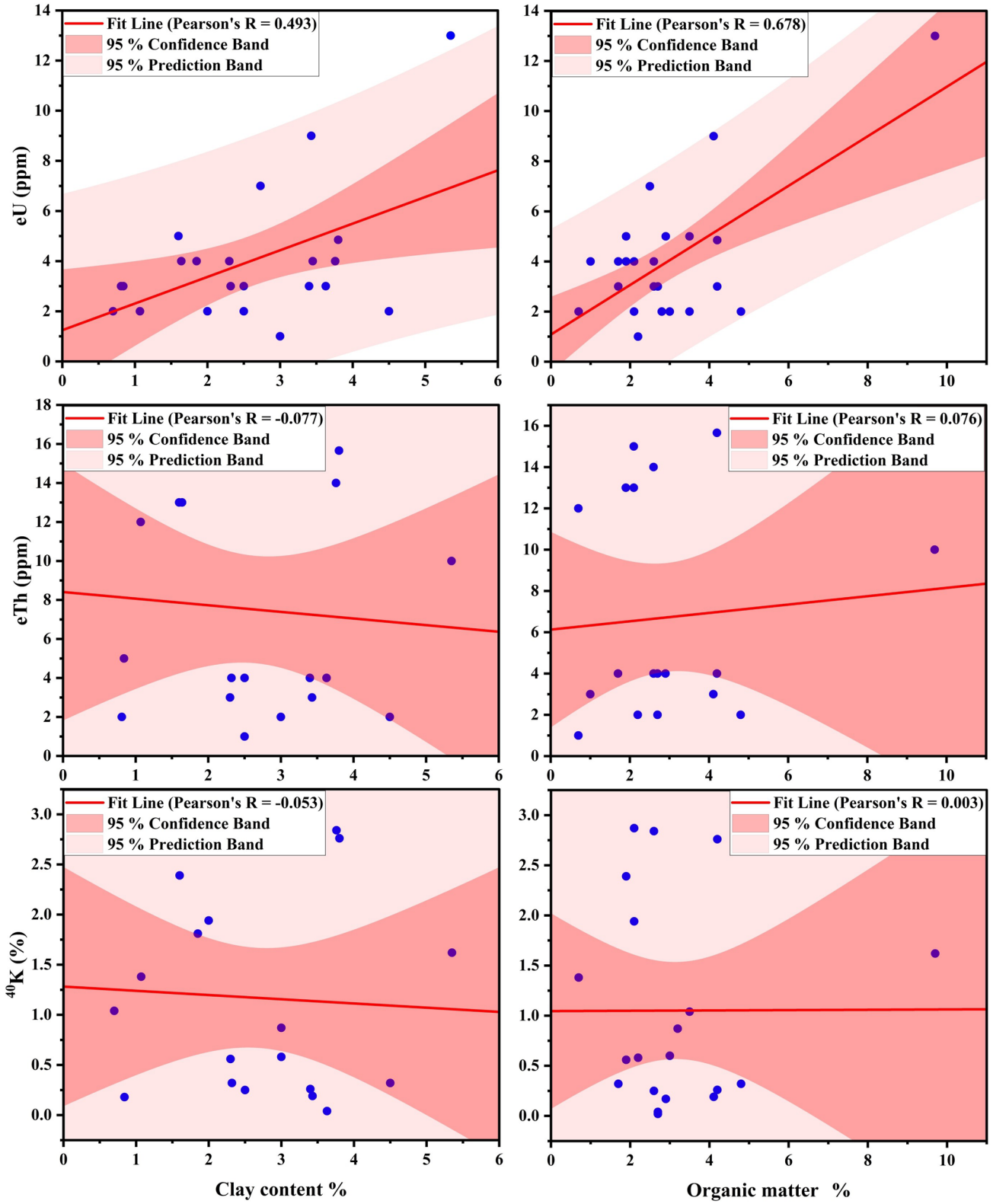

Fig. 9 Scatter plots showing the relationships between eU, eTh, and ^{40}K and the clay and organic matter contents %

Fig. 10 Field photograph showing uranyl minerals adsorbed on dark brown iron oxides in siltstone, Um Bogma Formation

extreme fractionation in uranium isotopes is attributed to excess ^{234}U alpha-recoil to groundwater as a result of ^{238}U decay in a uranium ore body. ^{238}U decays by emission of an alpha particle to ^{234}Th. A recoil energy is imparted to the resulting daughter thorium atom that may propel it distances on order of several angstroms through the mineral matrix (Kigoshi 1971). Since uranium concentrations in rocks generally exceeds groundwater concentrations by several orders of magnitude, recoil of ^{234}Th (which later decay to ^{234}U) from aquifer host rock to uranium poor groundwater is strongly favored (Osmond and Cowart 1976). This signifies that the relatively deep groundwater at El Allouga is being strongly depleted in ^{238}U while concomitantly being highly enriched in the ^{234}U isotope. It is most likely that U ore body could locally be forming within rock aquifer at El Allouga area. Such high uranium concentrations on rock surfaces would provide sources for recoil ^{234}U (Kronfeld 1974; Osmond and Cowart 1976; Andrews and Kay 1982). The highest activity ratio subsequently depends upon the prolonged residence time of the groundwater in the uraniferous zone of the aquifer and reflects uranium deposition from water. Conversely, if leaching and mobility of ^{238}U into the groundwater occurs this would result in decreasing the ^{234}U/^{238}U activity ratio of this water.

Radiation hazard and dose assessment

As shown in Table 2, the observed maximum value of Ra_{eq} in the studied stream sediments is 258.30 Bq kg^{-1}, which is lower than the safe maximum value (370 Bq kg^{-1}; UNSCEAR 2000). The calculated outdoor D_{ex}, AED_{ex} and ELCR values range from 0.00 to 120.14 nGy h^{-1} (mean 42.95 nGy h^{-1}), 0.00 to 0.147 mSv year^{-1} (mean 0.053 mSv year^{-1}) and 0.00×10^{-3} to 0.031×10^{-3} (mean 0.369×10^{-3}), respectively. These values are higher than the worldwide averages (57 nGy h^{-1}, 0.07 mSv year^{-1} and 0.29×10^{-3}, respectively; UNSCEAR 2000; UNSCEAR 2008; Taskin et al. 2009) in 30% of the studied stream sediment samples. This indicates that people who are receiving this exposure for a lifetime would have an elevated risk of cancer.

The calculated AED_{in} due to consumption of the studied water samples ranges from 0.004 to 0.0.050, 0.052 to 0.659, and 0.074 to 0.934 mSv year^{-1}, for infants, children, and adults, respectively (Table 3). It is evident that the AED resulting from U activity concentration in the studied drinking water was significantly higher than the recommended limit of 0.1 mSv year^{-1} (WHO 2011) for children and adults.

Conclusions

In the present study, the geochemical dispersion of radionuclides and their environmental impact in the vicinity of El Allouga uranium mine in southwestern Sinai were investigated. Generally, the following major conclusions can be obtained:

(1) Most of the studied stream sediments have eU concentration more than the uranium average of the earth's crust (2 ppm).
(2) eU is positively correlated with clay contents and organic matter contents. These correlations apparently reflect the adsorption of uranium to the surface of clay minerals and organic matter.
(3) The high concentrations of eU in some samples are mineralogically related to the presence of autunite, allanite, and xenotime.
(4) The high eU concentrations in the stream sediment samples located close to the mining area indicate a contamination from the mining process, whereas the weathering of rock outcrops in Wadi El Sahu contributes significantly to the radionuclide contents of the steam sediments
(5) The remarkable high concentrations of eTh in Wadi El Sahu stream sediments indicate derivation from the nearby granitic rocks. These high concentrations are mineralogically related to the existence of Th-bearing minerals in the concerned sediments.
(6) The concentrations of uranium in the groundwater of the study area are found to exceed the MCL of groundwater uranium.
(7) The general lack of correspondence of uranium concentrations in the groundwater and country rocks indicates that there does not exist a simple rock/water equilibration. This reflects that the high concentration of uranium in the groundwater of the study area is not mainly due to leaching from the nearby country rocks

Table 3 pH, TDS, major ions (mg/l), uranium concentrations (ppb) and $^{234}U/^{238}U$ activity ratios of the studied water samples and the calculated age-dependent internal dose

Sample no	pH	TDS (mg l^{-1})	Major ions (mg/l)							U (ppb)	$^{234}U/^{238}U$ Activity ratio	U in country rock (ppm)	AED (mSv yr^{-1})		
			Na^+	K^+	Ca^{2+}	Mg^{2+}	Cl^-	SO_4^{-2}	HCO_3^-				Infant	Children	Adults
1	8.01	1145.0	240.0	9.0	121.9	24.0	337.7	218.7	263.0	520.0	5.55 ± 0.69	2.47	0.023	0.303	0.430
2	8.02	1408.0	295.0	8.0	154.0	38.9	327.3	354.8	244.0	490.0	7.00 ± 0.82	NA	0.022	0.286	0.405
3	8.19	1600.0	294.0	11.0	201.0	39.0	414.6	478.0	204.0	510.0	3.34 ± 0.81	NA	0.022	0.297	0.422
4	8.15	2790.0	527.0	24.0	352.0	45.0	767.0	838.0	207.0	500.0	3.76 ± 0.71	NA	0.022	0.292	0.413
5	8.20	1043.0	211.0	7.0	98.0	43.4	259.5	228.0	229.0	420.0	14.00 ± 1.08	1706.00	0.019	0.245	0.347
6	8.18	992.0	201.0	7.0	96.1	27.0	235.8	201.0	256.0	470.0	6.73 ± 0.45	3.14	0.021	0.274	0.389
7	8.10	1600.0	304.0	8.0	158.0	35.9	434.3	360.0	200.0	90.0	4.07 ± 0.62	NA	0.004	0.052	0.074
8	8.07	1160.0	240.0	9.0	124.5	32.6	318.2	191.3	258.0	490.0	5.91 ± 0.37	NA	0.022	0.286	0.405
9	8.15	1267.0	267.0	9.0	108.0	21.1	356.0	253.0	185.0	510.0	3.41 ± 0.77	5.52	0.022	0.297	0.422
10	8.10	266.0	589.0	15.0	258.0	77.0	837.4	530.0	442.0	480.0	5.35 ± 0.48	4	0.021	0.280	0.397
11	7.90	12,096.0	3120.0	42.0	998.0	135.0	4798.7	2358.0	268.0	600.0	3.97 ± 0.33	NA	0.026	0.350	0.496
12	7.96	17,344.0	4325.0	78.0	1452.0	111.0	6584.0	3392.0	552.0	1130.0	4.31 ± 0.88	NA	0.050	0.659	0.934
Min	7.90	266.0	201.0	7.0	96.1	21.1	235.8	191.3	185.0	90.0	3.34 ± 0.81	–	0.004	0.052	0.074
Median	8.10	1337.5	294.5	9.0	156.0	38.9	385.3	357.4	250.0	495.0	4.83	–	0.022	0.289	0.409
Max	8.20	17,344.0	4325.0	78.0	1452.0	135.0	6584.0	3392.0	552.0	1130.0	14.00 ± 1.08	–	0.050	0.659	0.934
Mean	8.09	3559.3	884.4	18.9	343.5	52.5	1305.9	783.6	275.7	517.5	5.62	–	0.023	0.302	0.428
Std. deviation	0.10	5363.2	1355.7	21.2	429.5	36.1	2091.9	1018.3	109.5	229.6	2.92	–	0.010	0.134	0.190

NA not available

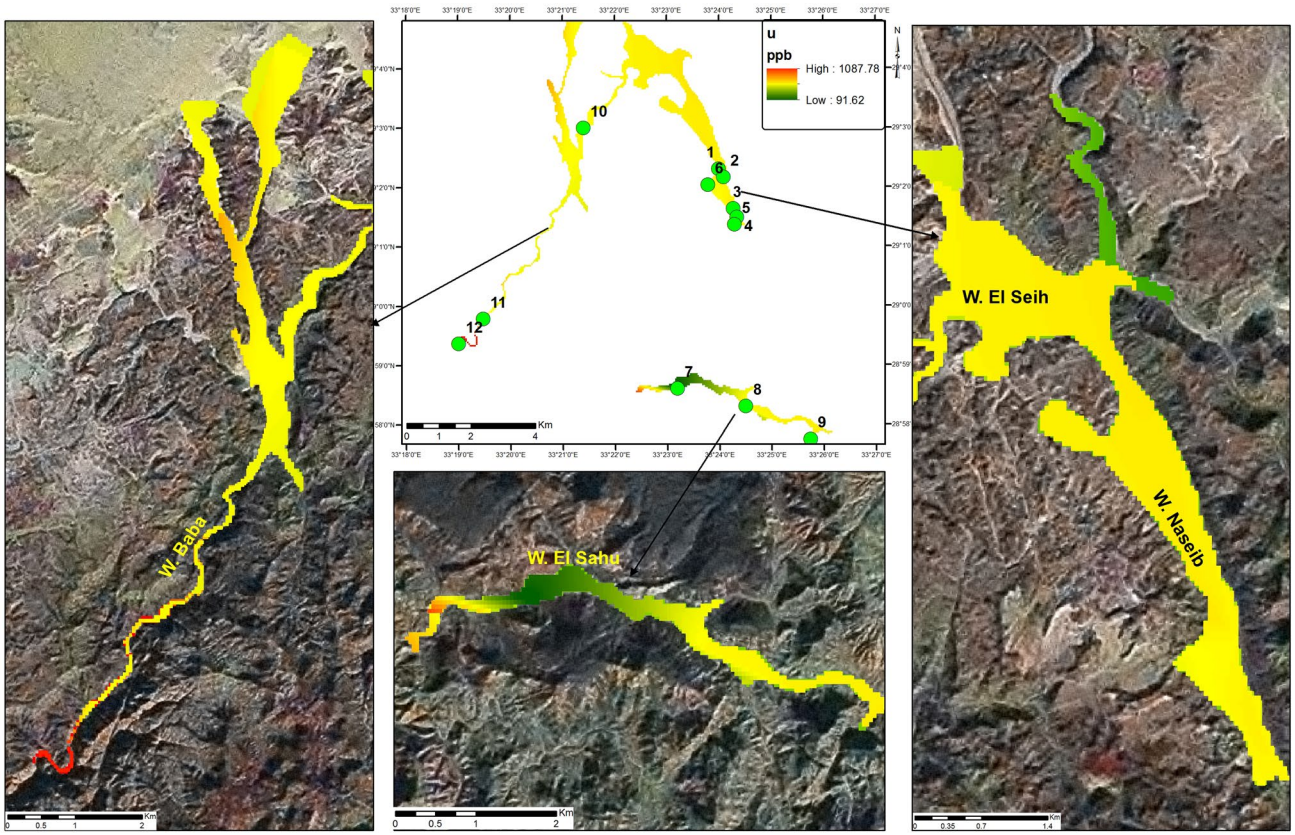

Fig. 11 Spatial distribution of U in the groundwater from studied wadis

and suggests that uranium in these aquifers has multi-sources due to its high mobility.

(8) Water samples have $^{234}U/^{238}U$ activity ratios with obvious deviations from secular equilibrium. It is most likely that U ore body could locally be forming within rock aquifer at El Allouga area, as evidenced by the very high $^{234}U/^{238}U$ activity ratio.

(9) The calculated external hazard parameter values are higher than the worldwide average in 30% of the studied stream sediment samples. This indicates that people who are receiving this exposure for a lifetime would have an elevated risk of cancer. The Annual Effective Dose resulting from U activity concentrations in the studied drinking water is significantly higher than the recommended limit for children and adults. Therefore, the available water resources in the study area are considered unsafe for human consumption.

(10) Consideration of the health impacts to the local indigenous populations needs to be carefully considered before permitting any expansion of the mining.

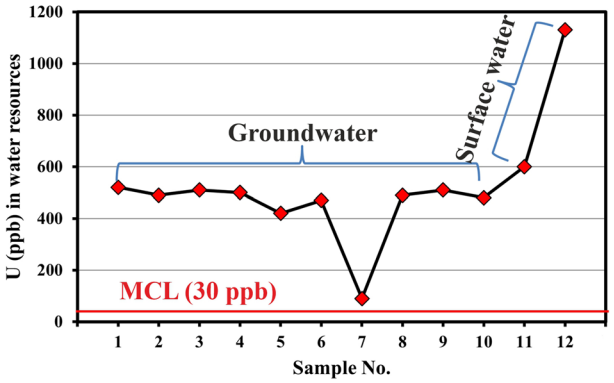

Fig. 12 Distribution of dissolved uranium in surface and groundwater from the study area

Table 4 Correlation matrix between uranium and major ions in the water samples

	U	TDS	Na^+	K^+	Ca^{2+}	Mg^{2+}	Cl^-	SO_4^{-2}	HCO_3^-
U	1	.786**	.788**	.845**	.797**	.571	.783**	.790**	.737**
TDS		1	.991**	.969**	.988**	.842**	.991**	.989**	.628*
Na^+			1	.970**	.994**	.890**	1.000**	.993**	.695*
K^+				1	.986**	.812**	.969**	.984**	.739**
Ca^{2+}					1	.881**	.994**	.999**	.698*
Mg^{2+}						1	.891**	.880**	.624*
Cl^-							1	.993**	.689*
SO_4^{-2}								1	.679*
HCO_3^-									1

** Correlation is significant at the 0.01 level (2-tailed); * Correlation is significant at the 0.05 level (2-tailed)

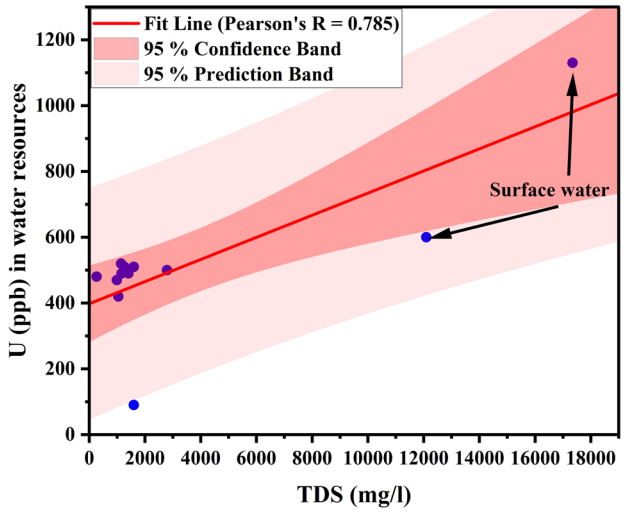

Fig. 13 Scatter plots showing the relationships between dissolved uranium and TDS

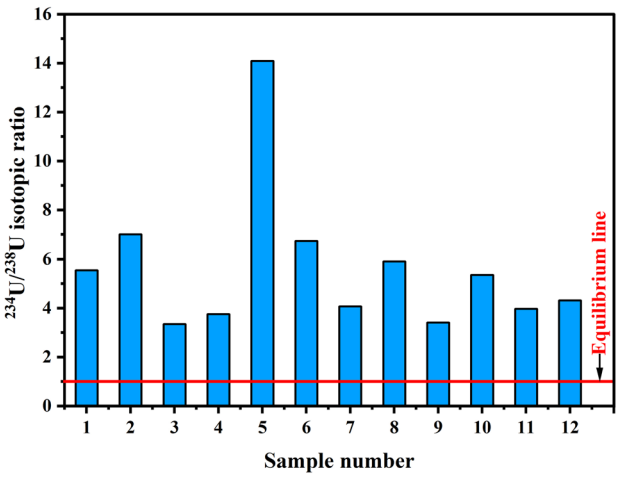

Fig. 15 Histogram showing the variations in activity ratio in the studied groundwater

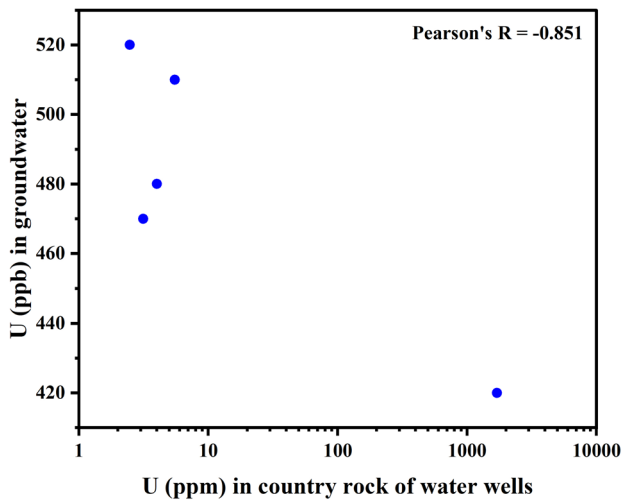

Fig. 14 The lack of correspondence between uranium in groundwater and country rocks

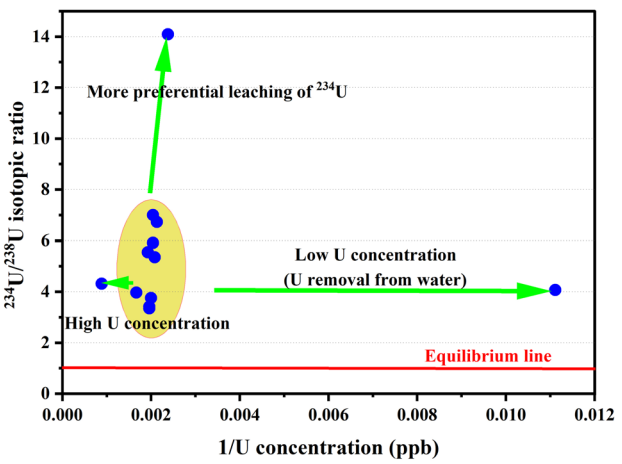

Fig. 16 Uranium activity ratio ($^{234}U/^{238}U$) as a function of reciprocal concentration (mixing diagram). All samples are in disequilibrium state. Explanations are written over arrows for extraordinary sample plots

Acknowledgements Mrs R. Ramadan would like to acknowledge laboratory facilities offered by Geology Department during her M.Sc. thesis. The authors wish to thank Prof. El Aassy I, Mr. Bahr S. (Nuclear Materials Authority), and Prof. Baghdady A (Ain Shams University) for their help in samples' collection; Dr. Kawady N and Mr. Bahr S (Nuclear Materials Authority) for their technical assistance. The authors are considerably grateful to the reviewers of this manuscript for their valuable comments and suggestions, which enabled us to improve the quality of the manuscript.

Author contributions Conceptualization: YD, AG, and RR; sampling: RR and AG; experimental and analyses: RR, AG and MY; data analysis: YD, AG, and RR; supervision: YD, MY, and AG; writing—original draft preparation: AG, and RR. Writing—review and editing: AG and YD. The manuscript was reviewed and approved for publication by all the authors.

Funding Open access funding provided by The Science, Technology & Innovation Funding Authority (STDF) in cooperation with The Egyptian Knowledge Bank (EKB). The authors did not receive support from any organization for the submitted work.

Availability of data and materials Not applicable.

Declarations

Conflict of interest The authors declare that they have no competing interests.

Ethics approval and consent to participate Not applicable.

Consent for publication Not applicable.

References

Abd El-Halim ES, Walley El-Dine N, El-Bahi SM, El Aassy IE, El-Sheikh EM, Al-Abrdi AM (2017) Excessive lifetime cancer risk and natural radioactivity measurements of granite and sedimentary rock samples. Nucl Phys Atom Energy 18(4):371–381. https://doi.org/10.15407/jnpae2017.04.371

Abdel-Monem AA, El Aassy IE, El-Naggar JM, Attia KE, El-Fawy AG (1996) Concentrations of radon gas and daughters in uranium exploration tunnels, Allouga, West Central Sinai, Egypt. Radiat Phys Chem 47(5):765–767. https://doi.org/10.1016/0969-806X(95)00173-U

Abdel-Razek YA, Masoud MS, Hanfi MY (2016) Effective radiation doses from natural sources at Seila area south Eastern Desert, Egypt. J Taibah Univ Sci 10:271–280. https://doi.org/10.1016/j.jtusci.2015.06.010

Aboelkhair H, Rabei M (2012) Radioelement mapping and environmental monitoring of surface deposits using ground gamma ray spectrometry of the area adjacent to El-Ramlah Village, Southwestern Sinai, Egypt. Resour Geol 62(2):215–224. https://doi.org/10.1111/j.1751-3928.2012.00190.x

Abu-zeid MM, El Kammar AM, El Aassy IE, Aly GA, Aita SK, Abu Zied EK, Abdel Azeem MM (2017) Mineral genesis and radioactivity of the upper part of the Adediya Formation, southwestern Sinai, Egypt. Ore Geol Rev 80:536–551. https://doi.org/10.1016/j.oregeorev.2016.06.003

Alshami AS (2018) U-minerals and REE distribution, paragenesis and provenance, Um Bogma Formation Southwestern Sinai, Egypt. Nucl Sci Sci J 7:31–55. https://doi.org/10.21608/nssj.2018.30721

Al-Sharkawy A, Hiekal MT, Sherif MI, Badran HM (2012) Environmental assessment of gamma-radiation levels in stream sediments around Sharm El-Sheikh, South Sinai, Egypt. J Environ Radioact 112:76–82. https://doi.org/10.1016/j.jenvrad.2012.05.020

Andrews JN, Kay RL (1982) $^{234}U/^{238}U$ activity ratios of dissolved uranium in groundwaters from a Jurassic Limestone aquifer in England. Earth Planet Sci Lett 57(1):39–151. https://doi.org/10.1016/0012-821X(82)90180-7

APHA (1995) Standard Methods: For the Examination of Water and Wastewater, APHA, AWWA, WEF/1995, APHA Publication

Benes P (1999) The environmental impacts of uranium mining and milling and the methods of their reduction. In: Choppin GR, Khankhasayev MKh (eds) Chemical separation technologies and related methods of nuclear waste management. Kluwer Academic Publishers, Dordrecht, pp 225–246. https://doi.org/10.1007/978-94-011-4546-6_13

Beretka J, Mathew PJ (1985) Natural radioactivity of Australian building materials, industrial wastes and by-products. Health Phys 48:87–95. https://doi.org/10.1097/00004032-198501000-00007

Blake JM, Avasarala S, Artyushkova K, Ali A-MS, Brearley AJ, Shuey C, Robinson WP, Nez C, Bill S, Lewis J, Hirani C, Pacheco JSL, Cerrato JM (2015) Elevated concentrations of U and co-occurring metals in abandoned mine wastes in a Northeastern Arizona Native American Community. Environ Sci Technol 49(14):8506–8514. https://doi.org/10.1021/acs.est.5b01408

Blake JM, Brown JE, Ferguson CL, Bixby RJ, Delay NT (2020) Sediment record of mining legacy and water quality from a drinking-water reservoir, Aztec, New Mexico, USA. Environ Earth Sci 79:404. https://doi.org/10.1007/s12665-020-09126-9

Borges RC, Mahler CF, Gomes AC, Balieiro F, Bellido AB, de Souza WL (2021) Radiological characterization of the area impacted by the Mariana dam disaster, in Mariana City-MG-Brazil. Environ Earth Sci 80:442. https://doi.org/10.1007/s12665-021-09649-9

Craft ES, Abu-Qare AW, Flaherty MM, Garofolo MC, Rincavage HL, Abou-Donia MB (2004) Depleted and natural uranium: chemistry and toxicological effects. J Toxicol Environ Health B Crit Rev 7(4):297–317. https://doi.org/10.1080/10937400490452714

Downing T, Moles J, McIntosh I, Garcia-Downing C (2002) Indigenous peoples and mining encounters: strategies and tactics. International Institute for Environment & Development, London

El Aassy IE, El Galy MM, Nada AA, El Feky MG, Abd El Maksoud TM, Talaat SM, Ibrahim EM (2011) Effect of alteration processes on the distribution of radionuclides in uraniferous sedimentary rocks and their environmental impact, southwestern Sinai, Egypt. J Radioanal Nucl Chem 289:173–184. https://doi.org/10.1007/s10967-011-1059-1

El Aassy IE, El-Feky MG, Issa FA, Ibrahim NM, Desouky OA, Khattab MR (2015) Uranium and $^{234}U/^{238}U$ isotopic ratios in some groundwater wells at Southwestern Sinai, Egypt. J Radioanal Nucl Chem 303:357. https://doi.org/10.1007/s10967-014-3461-y

El Galy MM, El Mezayn AM, Said AF, El Mowafy AA, Mohamed MS (2008) Distribution and environmental impacts of some radionuclides in sedimentary rocks at Wadi Naseib area, southwest Sinai, Egypt. J Environ Radioact 99:1075–1082. https://doi.org/10.1016/j.jenvrad.2007.12.012

El Mezayen AM, El-Balakssy SS, Abdel Ghani IM, El-Setouhy MS (2017) Radioactive mineralization of granitic rocks and their surrounding stream sediments at Gabal Rei El-Garrah area, Central Eastern Desert, Egypt. Nat Sci 15(12):61–78. https://doi.org/10.7537/marsnsj151217.06

El-kameesy SU, Afifi SY, Hamid A, Ajeeb A (2015) Elemental and radioactivity concentration of stream sediments in Abu-Rusheid, Nugrus Area—South Eastern Desert, Egypt. Am J Phys Appl 3(6):183–189. https://doi.org/10.11648/j.ajpa.20150306.11

Gad A, Saleh A, Khalifa M (2019) Assessment of natural radionuclides and related occupational risk in agricultural soil, southeastern Nile Delta, Egypt. Arab J Geosci 12:188. https://doi.org/10.1007/s12517-019-4356-6

Guagliardi I, Buttafuoco G, Apollaro C, Bloise A, De-Rosa R, Cicchella D (2013) Using gamma-ray spectrometry and geostatistics for assessing geochemical behavior of radioactive elements in the Lese Catchment (southern Italy). Int J Environ Res 7(3):645–658. https://doi.org/10.22059/IJER.2013.644

Hamby DM, Tynybekov AK (2000) Uranium, thorium and potassium in soils along the shore of lake Issyk-Kyol in the Kyrghyz Republic. Environ Monit Assess 73:101. https://doi.org/10.1023/A:1013071414970

Hanfi MY (2019) Radiological assessment of gamma and radon dose rates at former uranium mining tunnels in Egypt. Environ Earth Sci 78:113. https://doi.org/10.1007/s12665-019-8089-3

Harpy NM, El Dabour SE, Sallam AM, Nada AA, El Aassy AE, El Feky MG (2019) Radiometric and environmental impacts of mill tailings at experimental plant processing unit, Allouga, Egypt. Environ Forensics 21(1):11–20. https://doi.org/10.1080/15275922.2019.1695020

Hassan SF, Salam AM, Nasr MM, Mohamed WS (2015) Environmental impacts of radon and heavy metals in water wells and grasses from Wadi Sahu, South Western Sinai, Egypt. J Nucl Tech Appl Sci 3(3):145–155

Heikal MT, El-Dosuky BT, Ghoneim MF, Sherif MI (2013) Natural radioactivity in basement rocks and stream sediments, Sharm El Sheikh Area, South Sinai, Egypt: radiometric levels and their significant contributions. Arab J Geosci 6:3229. https://doi.org/10.1007/s12517-012-0622-6

Hund L, Bedrick EJ, Miller C, Huerta G, Nez T, Ramone S, Shuey C, Cajero M, Lewis J (2015) A Bayesian framework for estimating disease risk due to exposure to uranium mine and mill waste on the Navajo Nation. J R Stat Soc A 178:1069–1091. https://doi.org/10.1111/rssa.12099

Hussein HA, Abdel-Monem AA, Mahdy MA, El Aassy IE, Dabbour GA (1992) On the genesis of surficial uranium occurrences in West Central Sinai, Egypt. Ore Geol Rev 7:125–134. https://doi.org/10.1016/0169-1368(92)90008-9

IAEA (1996) International basic safety standards for protection against ionizing radiation and for the safety of radiation sources. Safety Report Series, No. 115, International Atomic Energy Agency

ICRP (1990) Recommendations of the International Commission on Radiological Protection, in ICRP Publication 60, Pergamon Press Ann ICRP, Oxford

ICRP (2012) Compendium of dose coefficients based on ICRP Publication 60. ICRP Publication 119. Ann. ICRP 41 (Suppl.)

Ingram RL (1971) Sieve analysis. In: Carver RE (ed) Procedures in sedimentary petrology. Jhon Wiley Intersciences, New York, pp 49–67

Ion A (2017) Natural radioactivity in stream sediments of Oltet River, Romania. Proceedings of the 19th EGU2017 conference, Vienna, Austria, 9965 p. https://ui.adsabs.harvard.edu/abs/2017EGUGA..19.9965I

Karpas Z, Paz-Tal O, Lorber A, Salonen L, Komulainen H, Auvinen A, Saha H, Kurttio P (2005) Urine, hair and nails as indicators for digestion of uranium in drinking water. Health Phys 88(3):229–242. https://doi.org/10.1097/01.HP.0000149883.69107.ab

Khattab MR, Ebyan OA, Abdel-rahman ME (2017) Distribution and disequilibrium of natural radionuclides in the black shale from Wadi Naseib area, Southwest Sinai, and their environmental hazard indices. Radiat Prot Environ 40(3):126–132. https://doi.org/10.4103/rpe.RPE_23_17

Kigoshi K (1971) Alpha-recoil thorium-234: dissolution into water and the uranium-234/uranium-238 disequilibrium in nature. Science 173(3991):47–48. https://doi.org/10.1126/science.173.3991.47

Kora M, El Shahat A, Abu Shabana M (1994) Lithostratigraphy of the manganese-bearing Urn Bogma Formation, west-central Sinai, Egypt. J Afr Earth Sci 18(2):151–162. https://doi.org/10.1016/0899-5362(94)90027-2

Korany KA, Shata AE, Hassan SF, Nagdy MS (2013) Depth and seasonal variations for the soil radon-gas concentration levels at Wadi Naseib area, Southwestern Sinai, Egypt. J Phys Chem Biophys 3(4):123. https://doi.org/10.4172/2161-0398.1000123

Kronfeld J (1974) Uranium deposition and ^{234}Th alpha-recoil: an explanation for extreme ^{234}U/^{238}U fractionation within the Trinity Aquifer. Earth Planet Sci Lett 21(3):327–330. https://doi.org/10.1016/0012-821X(74)90169-1

Langmuir D (1978) Uranium solution-mineral equilibria at low temperatures with applications to sedimentary ore deposits. Geochim Cosmochim Acta 42:547–569. https://doi.org/10.1016/0016-7037(78)90001-7

Lewis J, Hoover J, MacKenzie D (2017) Mining and environmental health disparities in native American communities. Curr Environ Health Rep 4:130–141. https://doi.org/10.1007/s40572-017-0140-5

Lima A, Albanese S, Cicchella D (2005) Geochemical baselines for the radioelements K, U, and Th in the Campania region, Italy: a comparison of stream-sediment geochemistry and gamma-ray surveys. Appl Geochem 20:611–625. https://doi.org/10.1016/j.apgeochem.2004.09.017

Ma M, Wang R, Xu L, Xu M, Liu S (2020) Emerging health risks and underlying toxicological mechanisms of uranium contamination: lessons from the past two decades. Environ Int 145:106107. https://doi.org/10.1016/j.envint.2020.106107

Mange MA, Maurer HW (1992) Methods. In: Mange MA, Maurer HW (eds) Heavy minerals in colour. Chapman Hall, London, pp 11–25. https://doi.org/10.1007/978-94-011-2308-2_3

NEA (2004) Uranium 2003: Resources, Production and Demand, A Joint Report by the OECD Nuclear Energy Agency and the International Atomic Energy Agency, OECD, Paris, NEA No. 5291

NEA (2014) Uranium 2014: Resources, Production and Demand, A Joint Report by the OECD Nuclear Energy Agency and the International Atomic Energy Agency, OECD, Paris, NEA No. 7209

Orgün Y, Altinsoy N, Sahin SY, Gungor Y, Gultekin AH, Karaham G, Karaak Z (2007) Natural and anthropogenic radionuclides in rocks and beach sands from Ezine region (canakkale), Western Anatolia, Turkey. Appl Radiat Isot 65:739–747. https://doi.org/10.1016/j.apradiso.2006.06.011

Osman R, Dawood YH, Melegy A, El-Bady MS, Saleh A, Gad A (2022) Distributions and risk assessment of the natural radionuclides in the soil of Shoubra El Kheima, South Nile Delta, Egypt. Atmosphere 13:98. https://doi.org/10.3390/atmos13010098

Osmond JK, Cowart JB (1976) The theory and uses of natural uranium isotopic variations in hydrology. At Energy Rev 14(4):621–679

Osmond JK, Cowart JB (1992) Groundwater. In: Ivanovich M, Harmon R (eds) Uranium series disequilibrium: application to environmental problems, 2nd edn. Clarendon Press, pp 290–333

Ramadan SR, Gad A, Yehia MM, Dawood YH, Kawady NA (2019) Grain size and mineralogical characteristics of the stream sediments, east of Abu Zeneima area, southwestern Sinai, Egypt. Arab J Geosci 12:192. https://doi.org/10.1007/s12517-019-4362-8

Refaei AM, El-Nennah ME, Khaled EM, Abd El-Fattah NA (2019) Environmental contamination by heavy metals and radioactive elements in Wadi Nasab and its surroundings, Southwestern Sinai, Egypt. Arab Univ J Agric Sci 27(4):2341–2351. https://doi.org/10.21608/ajs.2019.17558.1094

Schultz R (2021) Investigating the health impacts of the Ranger uranium mine on Aboriginal people. Med J Aust 215:157-159.e1. https://doi.org/10.5694/mja2.51198

Sturchio NC, Banner JL, Binz CM, Heraty LB, Musgrove M (2001) Radium geochemistry of ground waters in Paleozoic carbonate aquifer, midcontinent, USA. Appl Geochem 16:109–122. https://doi.org/10.1016/S0883-2927(00)00014-7

Suzuki Y, Banfield JF (1999) Geomicrobiology of uranium. Rev Mineral Geochem 38(1):393–432

Taskin H, Karavus M, Ay P, Topuzoglu A, Hindiroglu S, Karahan G (2009) Radionuclide concentrations in soil and lifetime cancer risk due to the gamma radioactivity in Kirklareli, Turkey. J Environ Radioact 100:49–53. https://doi.org/10.1016/j.jenvrad.2008.10.012

Taylor SR (1964) Abundance of chemical elements in the continental crust; a new table. Geochim Cosmochim Acta 28(8):1273–1285. https://doi.org/10.1016/0016-7037(64)90129-2

UNSCEAR (2000) Sources and Effects of Ionizing Radiation, Report to the General Assembly with Scientific Annexes. United Nation, New York

UNSCEAR (2008) Sources and Effects of Ionizing Radiation. Report to the General Assembly with Scientific Annexes. United Nations, New York

Van Reeuwijk LP (2002) Procedures for soil analysis, 6th edn. International Soil Reference and Information Centre, Wageningen

WHO (2011) Guidelines for drinking water quality, 4th edn. Switzerland: Geneva

Winde F, Brugge D, Nidecker A, Ruegg U (2017) Uranium from Africa—an overview on past and current mining activities: re-appraising associated risks and chances in a global context. J Afr Earth Sci 129:759–778. https://doi.org/10.1016/j.jafrearsci.2016.12.004